

# ENHANCING EFFECTIVE THERMAL CONDUCTIVITY PREDICTIONS IN DIGITAL POROUS MEDIA USING TRANSFER LEARNING

Mohamed Elmorsy<sup>1</sup>, Wael El-Dakhakhni<sup>1,2</sup>, Benzhong Zhao<sup>1</sup>

<sup>1</sup>Department of Civil Engineering, McMaster University, Hamilton, ON, Canada; <sup>2</sup>School of Computational Science & Engineering, McMaster University, Hamilton, ON, Canada

# Correspondence to:

Benzhong Zhao,

robinzhao@mcmaster.ca

#### **How to Cite:**

ipj.v2i3nr75

Elmorsy, M., El-Dakhakhni, W., & Zhao, B. (2025). Enhancing
Effective Thermal
Conductivity Predictions
in Digital Porous Media
Using Transfer Learning.
InterPore Journal, 2(3),
IPJ250825-7.
https://doi.org/10.69631/

RECEIVED: 3 Feb. 2025 ACCEPTED: 12 May 2025 PUBLISHED: 25 Aug. 2025

#### **ABSTRACT**

Porous media beneath the Earth's surface, including aquifers, oil and gas reservoirs, and geothermal systems, play a crucial role in various natural resource management and environmental engineering applications. The study of their physical properties, particularly thermo-physical properties like effective thermal conductivity (ETC), is essential for enhancing the efficiency of subsurface engineering technologies including nuclear waste disposal, geothermal energy utilization, and underground thermal energy storage. Traditionally, determining ETC has relied on either simplified empirical models, which often lack accuracy, or sophisticated laboratory experiments, which are time-consuming and resource intensive. The advent of threedimensional (3D) imaging technologies has enabled digital characterization of subsurface media, but direct numerical simulations of ETC remain computationally prohibitive. In response to these challenges, we introduce a novel machine learning framework that leverages transfer learning to enhance the prediction of ETC in digital rock samples. Our approach utilizes state-of-the-art convolutional neural networks (CNNs), pre-trained on extensive datasets, and applies them to various porous media samples, including Berea sandstone, Bentheimer sandstone, and Ketton limestone. By employing transfer learning, we demonstrate that our models can achieve high prediction accuracy with significantly reduced training time, computational power, and data requirements. This study highlights the potential of transfer learning to advance the efficiency and accuracy of digital rock analysis, offering a promising tool for the rapid and reliable characterization of subsurface properties.

# **KEYWORDS**

Digital rock physics, Machine learning, Geothermal energy, Effective thermal conductivity



This is an open access article published by InterPore under the terms of the Creative Commons Attribution-NonCommercial-NoDerivatives 4.0 International License (CC BY-NC-ND 4.0) (https://creativecommons.org/licenses/by-nc-nd/4.0/).

# 1. INTRODUCTION

Porous media beneath the Earth's surface, including aquifers, oil and gas reservoirs, and geothermal systems, are integral to various natural resource and environmental management applications. The physical properties of these media have been extensively studied to elucidate their behavior and facilitate

Elmorsy et al. Page 2 of 19

the development of predictive models for flow and transport phenomena. Among these properties, thermo-physical characteristics, particularly the effective thermal conductivity (ETC)—which represents the thermal conductivity of the geological porous medium—are crucial in subsurface engineering technologies including nuclear waste disposal (29), geothermal energy utilization (35), underground thermal energy storage (61), and enhanced oil recovery (48). The thermal conductivity of the porous media is a critical parameter in evaluating the performance and safety of these subsurface technologies (69). Thermal conductivity is the measure of how efficiently heat passes through a material given a unit temperature difference across a unit area of the material with a unit thickness, under steadystate conditions (44). In porous media, thermal conductivity is not a fixed value; it varies as a function of factors such as porosity, water saturation, mineralogical composition, and most notably, the pore microstructure and temperature of the medium (1). Consequently, the thermal conductivity of porous media, such as rocks, is termed effective thermal conductivity (2, 69). In the case of dry sedimentary rocks, the thermal conductivity of air (approximately 0.026 W/m·K) within the pores is significantly lower compared to that of the solid rock matrix (ranging from 0.4 to 7 W/m·K). Therefore, the microstructure of the pores, including their volume, shape, and distribution, plays a fundamental role in determining the ETC of the rock samples (44).

The determination of ETC of porous media includes conducting laboratory and field experiments as well as developing theoretical models. Experimental techniques, including needle probes (25, 74), guarded parallel plates (1), and optical scanning (55), are commonly employed to measure the ETC of porous media. However, these experimental methods are often costly, requiring specialized equipment, materials, and skilled personnel. Additionally, the experimental process is time-intensive, requiring extensive preparation, data collection, and analysis, which can impede the research progress and limit the number of experiments that can be feasibly conducted (83). To mitigate these challenges, analytical methods such as the Maxwell model and the weighted harmonic mean equation offer a more rapid approach to estimating the ETC. These methods provide simple analytical formulas that can predict the effective thermal conductivity of porous media using only the volume fraction of the sample (9, 35). However, despite their ease of use, these analytical models tend to oversimplify the complex structural characteristics of porous media, leading to limitations in their accuracy (21). The intricate pore structures and irregular pore distributions within porous media create significant challenges, and as a result, a universally accepted analytical relationship between ETC and geometric structural parameters remains elusive (81).

In recent years, digital rock physics technology has been widely adopted for simulating the physical properties of porous media, thanks to its benefits in digitalization and visualization (49). Progress in imaging technologies, including X-ray micro-computed tomography (15), neutron tomography (51), and micro-positron tomography (80) have enabled the visualization of the three-dimensional (3D) internal structure of porous media that are otherwise opaque. These imaging techniques facilitate the digital characterization of the physical properties of porous media through numerical simulations (7, 8, 13). Two types of simulation approaches are commonly employed: pore network modeling and direct numerical modeling. Pore network models utilize simplified geometries, such as spheres and cylinders, to represent the pores and throats within porous media. In contrast, direct numerical models create meshes from digitized image blocks, offering a more precise representation of the complex microstructure in porous media (65). Direct numerical simulations, including those employing the finite element method (FEM) and the finite volume method (FVM), are developed based on physical modeling by solving partial differential equations and are effectively used for simulating flow and heat transfer within micro-CT images of digital rocks (19, 70). These simulation techniques allow for a more accurate and detailed analysis of the internal structure and properties of porous media (65), contributing to a deeper understanding of flow and heat transfer under various conditions (47).

For example, Yang et al. (79) evaluated the effects of fracture parameters—such as length, aperture, and angle—on the thermal conductivity of digital rocks, using  $50 \times 50 \times 50$  cubic voxel samples reconstructed from a stack of 2D images of sandstone with varying fractures. Similarly, Dongxing et al. (21) developed a digital model of a homogeneous rock by performing a 3D reconstruction of its internal

Elmorsy et al. Page 3 of 19

structure using a series of micro-CT images. By generating high-quality meshes compatible with computational fluid dynamics (CFD) software, they calculated the ETC of rock samples of varying sizes in three directions through direct numerical simulation. The study concluded that digital rock analysis offers a feasible and reliable alternative for evaluating the thermal properties of rocks, grounded in the accurate characterization of the internal microscale structure of porous media. However, performing direct numerical simulations of thermal transport in 3D porous media remains computationally intensive, requiring significant computing power and memory resources (20).

Recently, machine learning has emerged as a powerful tool for the digital characterization of subsurface porous media, offering significant advantages in terms of efficiency by reducing the time and computational costs associated with analyzing large datasets (52). Machine learning algorithms are particularly effective at identifying complex patterns and relationships within data, leading to accurate predictions of key properties, including the thermo-physical properties of porous media. For instance, Vaferi et al. (73) employed a two-layer artificial neural network (ANN) to estimate the ETC of dry and oil-saturated sandstone under a wide range of environmental conditions. The predicted ETC values showed strong agreement with experimental thermal conductivity data, with absolute average relative deviation percentages of 2.73% and 3.81% for the overall experimental dataset of oil-saturated and dry sandstone, respectively.

Fei et al. (25) utilized micro-CT images of four dry sand samples to predict their ETC using an artificial neural network (ANN) model with pre-calculated micro-structural parameters. In their approach, the sand is represented as a network composed of nodes (sand grains) and edges (inter-grain contacts or small gaps between neighboring grains). In particular, the weighted coordination number, which accounts for both particle connectivity and contact area, was identified as a particularly reliable predictor of ETC in dry materials. The model demonstrated good predictive capabilities, achieving a high correlation ( $R^2 = 0.97$ ) between the predicted and actual ETC values obtained through thermal needle probe testing. Similarly, Wei et al. (75) employed pre-calculated features to predict the ETC of digital porous media by investigating structural characteristics that significantly impact thermal transport. To effectively describe the characteristics of porous media, they devised five structural descriptors: shape factor, bottleneck, channel factor, perpendicular non-uniformity, and dominant paths. These descriptors were then utilized in two conventional machine learning models—support vector regression (SVR) and Gaussian process regression (GPR)—to predict the ETC of porous media. Specifically, both models were trained on a dataset comprising 2,460 synthetic 2D porous media images, each  $100 \times 100$  pixels in size, generated using the quartet structure generation set (QSGS) technique. The models were then tested on  $615\ 100 \times 100$  images. The predicted thermal conductivity values from the machine learning models were comparable to those estimated by FEM simulations, with most absolute relative prediction errors within a 30% range.

Unlike ANNs that rely on pre-calculated features as input, convolutional neural networks (CNNs) represent a more advanced deep learning method that enables end-to-end predictions by accepting 2D and 3D images directly as input. Convolutional neural networks have been extensively utilized in various computer vision applications, such as face recognition (36, 38) and object detection (26, 84), due to their ability to automatically extract relevant features from input images. Similarly, CNNs have been widely employed in digital porous media studies to automatically extract internal microstructural features and determine their relationship with the effective properties being analyzed (22, 23, 37, 78). In the context of ETC prediction, Wei et al. (76) introduced a machine learning framework incorporating SVR, GPR, and CNN models to investigate heat transport in digital porous media and found that they yielded more accurate predictions compared to traditional analytical models, such as the Maxwell-Eucken and Bruggeman models. Furthermore, they concluded that, given a sufficiently robust training dataset, machine learning techniques offer a valuable and efficient means for predicting the ETC of porous media. In another study, Rong et al. (57) explored the application of 2D and 3D CNNs for predicting the ETC of digital porous media. They generated a synthetic 3D porous media dataset using particle-packing and QSGS techniques, creating a training dataset of 2,000 100 × 100 × 100 sub-volumes with a fixed solid

Elmorsy et al. Page 4 of 19

volume fraction of 0.35, for which the ETC was simulated using the FEniCS software<sup>a</sup>. Initially, they trained a 2D CNN based on the AlexNet (42) architecture to predict the ETC of the 3D samples. Subsequently, they investigated the use of a 3D CNN for training on the dataset. However, due to the high computational demands of training 3D CNNs, they were required to reduce the dataset size to 800 samples and simplify the 3D CNN architecture to just three convolutional layers. While the CNN models produced results comparable to those obtained from numerical simulations and achieved low mean absolute error (MAE) and root mean square error (RMSE) values, both below 5%, the training process was still time-consuming, taking six days on a single CPU.

Traditionally, training deep learning models such as CNNs require a vast amount of training data, which poses a significant challenge in practical applications where available datasets are often limited and sparse. This limitation restricts the broader use of deep learning in various domains. To address this issue, a new branch of machine learning known as Transfer Learning has emerged. Transfer learning is a powerful machine learning technique, enabling models to leverage pre-trained knowledge to improve performance on new tasks with limited data (3, 66). It works by transferring knowledge acquired by a model trained on one task or domain to enhance performance on a related but distinct task (77). By reusing the weights of pre-trained models, transfer learning accelerates training, improves predictive accuracy, and reduces reliance on large datasets (24). This approach has been successfully applied across numerous fields. In medical imaging, for example, fine-tuning pre-trained models on domain-specific datasets has significantly improved cancer detection and neurological disorder classification (5, 64). Architectures such as ResNet and VGGNet have shown strong performance by reducing training time and addressing class imbalances (41, 60). In natural language processing (NLP), models like BERT and GPT leverage transfer learning to achieve superior results in tasks such as text classification and machine translation, benefiting from the efficiency of transformer-based architectures (10, 58). Autonomous driving systems also employ transfer learning to bridge the gap between simulation and real-world environments, improving collision avoidance and domain adaptation through deep reinforcement learning and federated transfer learning (40, 45, 72). In materials science and geophysics, transfer learning enables accurate property predictions from limited data, with cross-property deep transfer learning often outperforming traditional approaches (30, 31). These diverse applications underscore the versatility of transfer learning, accelerating discovery and improving computational efficiency across disciplines.

Convolutional neural networks models such as VGG (63), Inception (67), and ResNet (32), all trained on the ImageNet dataset, have proven highly effective in transfer learning applications. Their pre-trained architecture provides robust feature extraction capabilities, making them invaluable in scenarios where acquiring large-scale labeled datasets is challenging or costly, such as medical image analysis. Consequently, many studies in the medical field have reported the successful application of transfer learning techniques (17, 34, 68). For example, Michał Byra et al. (18) utilized a pre-trained Inception-ResNet-v2 CNN, originally trained on the ImageNet dataset, to extract high-level features from liver Bmode ultrasound images. These extracted features were then used by a support vector machine (SVM) algorithm to categorize images with fatty liver, a clinically relevant step in determining the grade of liver steatosis. In the context of digital rock analysis, Liu et al. (46) applied transfer learning to estimate the effective permeability of digital rocks. Specifically, they employed the VGG pre-trained model to extract salient features from micro-CT images of sandstone and carbonate samples that are most sensitive to permeability. The predicted permeabilities using this approach were consistent with direct numerical simulation results while significantly reducing computational time and memory requirements compared to traditional direct numerical simulations.

Here, we introduce a novel approach to characterize the ETC of digital porous media by leveraging transfer learning. Our machine learning framework employs four pre-trained CNN models as feature extractors for 3D images of digital rocks, significantly expediting the training process, reducing the need for large datasets, and minimizing computational resource demands while maintaining high accuracy.

a https://fenicsproject.org/

Elmorsy et al. Page 5 of 19

We anticipate that the use of transfer learning has the potential to revolutionize the digital characterization of porous media, particularly in cases where 3D image datasets are scarce. Even when large datasets of 3D images become available, training complex deep learning models from scratch requires substantial computational resources, both in terms of processing power (e.g., multiple GPUs) and time (e.g., training that can extend to days or even weeks). Consequently, this approach paves the way for more efficient prediction, analysis, and understanding of porous media properties (e.g., permeability, electrical resistivity, elastic modulus) using machine learning with fewer resources and at greater speeds.

# 2. METHODOLOGY

# 2.1. Data Preparation and Processing

We created our machine learning models using a dataset of 3D images of various digital porous media samples, which are publicly accessible (**Table 1**). These images were originally obtained by researchers at Imperial College London using synchrotron X-ray beamlines or micro-CT scanners. This dataset has been employed in prior studies to examine different pore-scale flow and transport processes in digital porous media (15, 50).

Table 1: Digital rock samples used for training and testing the machine learning methods.						
Rock type	Size (mm)	Resolution (µm/voxel)	Porosity (-)	Stride (voxel)	Number of subvolumes (-)	Number of labelled ETC (-)
Bentheimer sandstone	3	3	0.22	50	4,877	14,631
Ketton limestone	3	3	0.13	50	3,819	11,457
Berea sandstone	2.1	5.3	0.19	25	4,651	13,953
ETC: effective thermal conductivity						

The dataset is stored and made publicly accessible through an online portal (14). We utilized three sets of 3D scans from cores of Bentheimer sandstone, Berea sandstone, and Ketton limestone. The 3D images of Bentheimer sandstone and Ketton limestone consist of  $1000 \times 1000 \times 1000$  cubic voxels with a resolution of 3 µm/voxel, while the Berea sandstone core measures  $400 \times 400 \times 400$  cubic voxels with a resolution of 5.3 µm/voxel. To maintain consistency in the scale of all samples in our study, we rescaled the Berea sandstone images to  $712 \times 712 \times 712$  cubic voxels, ensuring that each voxel corresponds to a physical dimension of 3 µm (**Fig. 1**). The rescaling procedure was validated by comparing the porosity of the rescaled sample to that of the original, revealing a variation of less than 2%, which confirmed the effectiveness of the rescaling technique. Then, we extracted subvolumes from the 3D images using a sliding cube of  $150 \times 150 \times 150 \times 150$  cubic voxels, with an overlapping stride of either 25 or 50 voxels (**Table 1, Fig. 1**).

We employed OpenFOAM<sup>b</sup>, an open-source suite of CFD solvers (33), to numerically simulate the thermal conductivity of the extracted subvolumes. OpenFOAM simulates heat conduction by solving Fourier's law (**Eq. 1**), where q is the heat flux,  $\lambda$  is the thermal conductivity, and  $\nabla T$  is the temperature gradient.

$$q = -\lambda \nabla T \tag{1}$$

We simulated heat conduction along each of the principal axis (i.e., x, y, z) of the porous media samples. Specifically, a fixed heat flux was applied at the heat input surface, and a fixed temperature was maintained at the heat output surface. The laplacian FOAM algorithm was then employed to compute the temperature at the inlet surface. Finally, the thermal conductivity of the porous media sample was

\_

b https://www.openfoam.com/

Elmorsy et al. Page 6 of 19

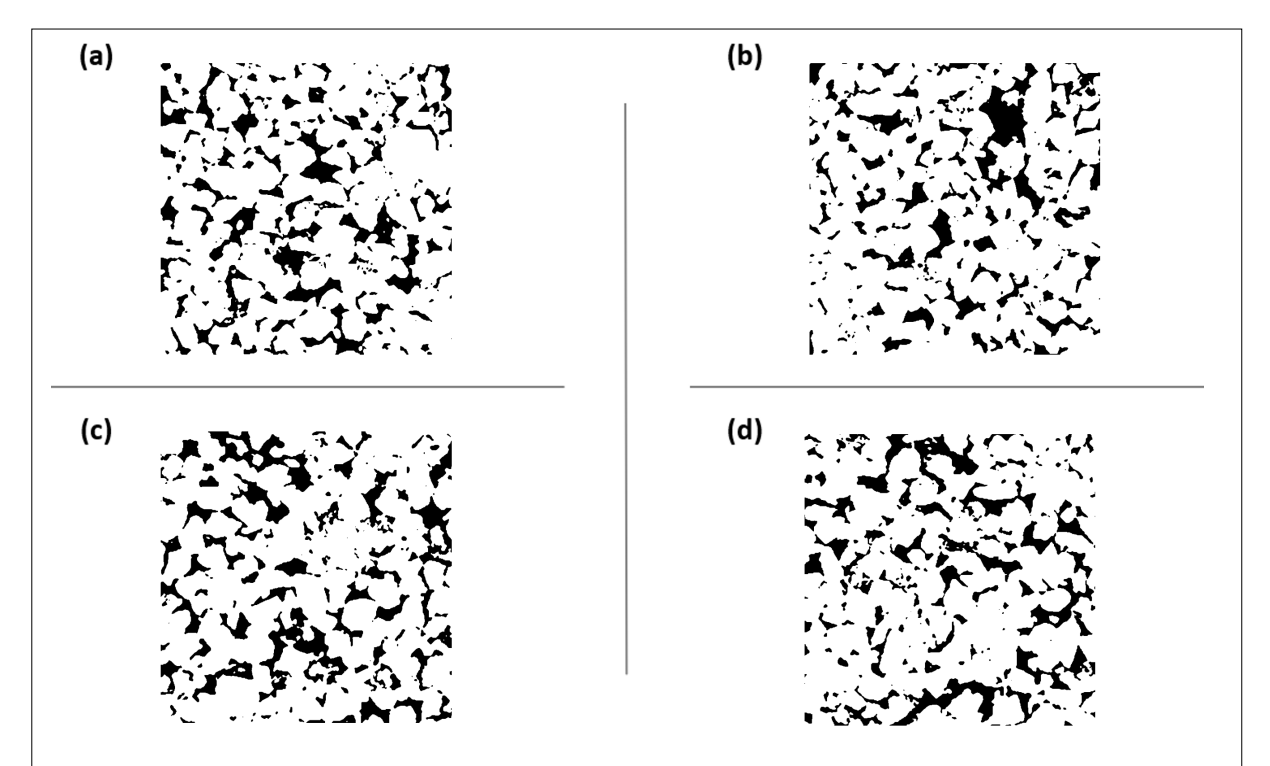


**Figure 1:** Sample sequential 2D slices from a 3D  $\mu$ CT scan of Berea sandstone after rescaling, where **(a)** shows the  $1^{st}$  slice, **(b)** the  $200^{th}$  slice, **(c)** the  $400^{th}$  slice, and **(d)** the  $600^{th}$  slice. The void (pore) spaces of the porous medium are shown in black, and the solid matrix is shown in white.

calculated using **Equation 2**, where  $q_t$  is the total heat transfer rate integrated over the entire input surface,  $S_{in}$  is the area of the input surface,  $T_{in}$  and  $T_{out}$  are the inlet and outlet temperature, respectively, and L is the distance between the inlet and the outlet surfaces of the sample.

$$\lambda = \frac{q_{\rm t}L}{S_{\rm in}(T_{\rm in} - T_{\rm out})} \tag{2}$$

Although the thermal conductivity for the solid phase  $\lambda_s$  varies depending on the material, we set  $\lambda_s$  to unity (i.e,  $\lambda_s = 1 \text{ W/m} \cdot \text{K}$ ) for all simulations, and report the ETC as  $\lambda_{\text{eff}} = \lambda/\lambda_s$ .

We conducted over 40,000 simulations on a dataset of  $150 \times 150 \times 150$  subvolumes, which were randomly split into training and testing sets in a 90-10 ratio (**Fig. 2a, b**). In our methodology, the ETC values obtained from numerical simulations serve as the ground truth labels for training and testing the machine learning models, providing the reference against which the models' predictive capabilities are evaluated. To enhance the training set, we implemented data augmentation techniques. Common methods for data augmentation in machine learning include simple image transformations such as flipping and rotating. For example, Elmorsy et al. (22) utilized image flipping to effectively increase the size of their digital rocks training dataset, resulting in improved accuracy and generalizability of their model. Similar techniques have been applied to benchmark datasets like ImageNet and CIFAR-10 (62). In our study, we generated four unique subvolumes with the same effective thermal conductivity (ETC) value by horizontally and vertically flipping the individual 2D image slices that constitute each 3D subvolume. Additionally, we reversed the order of the 2D slices to create four more distinct subvolumes with the same ETC value. This augmentation process expanded the original training dataset to approximately 288,000 distinct subvolumes, encompassing around 36,000 unique ETC values.

The ETC values in the dataset span from 0.38 to 0.98 and display a negatively skewed distribution, with a tail extending toward the lower ETC region (**Fig. 2c**). Such skewed distributions are common in natural phenomena, such as rainfall and earthquakes; however, they pose significant challenges for machine learning models. Algorithms often interpret the "tail" of the distribution as outliers, which can result in biased predictions that favor the more prevalent values in the training data (11, 53). This bias impedes

Elmorsy et al. Page 7 of 19

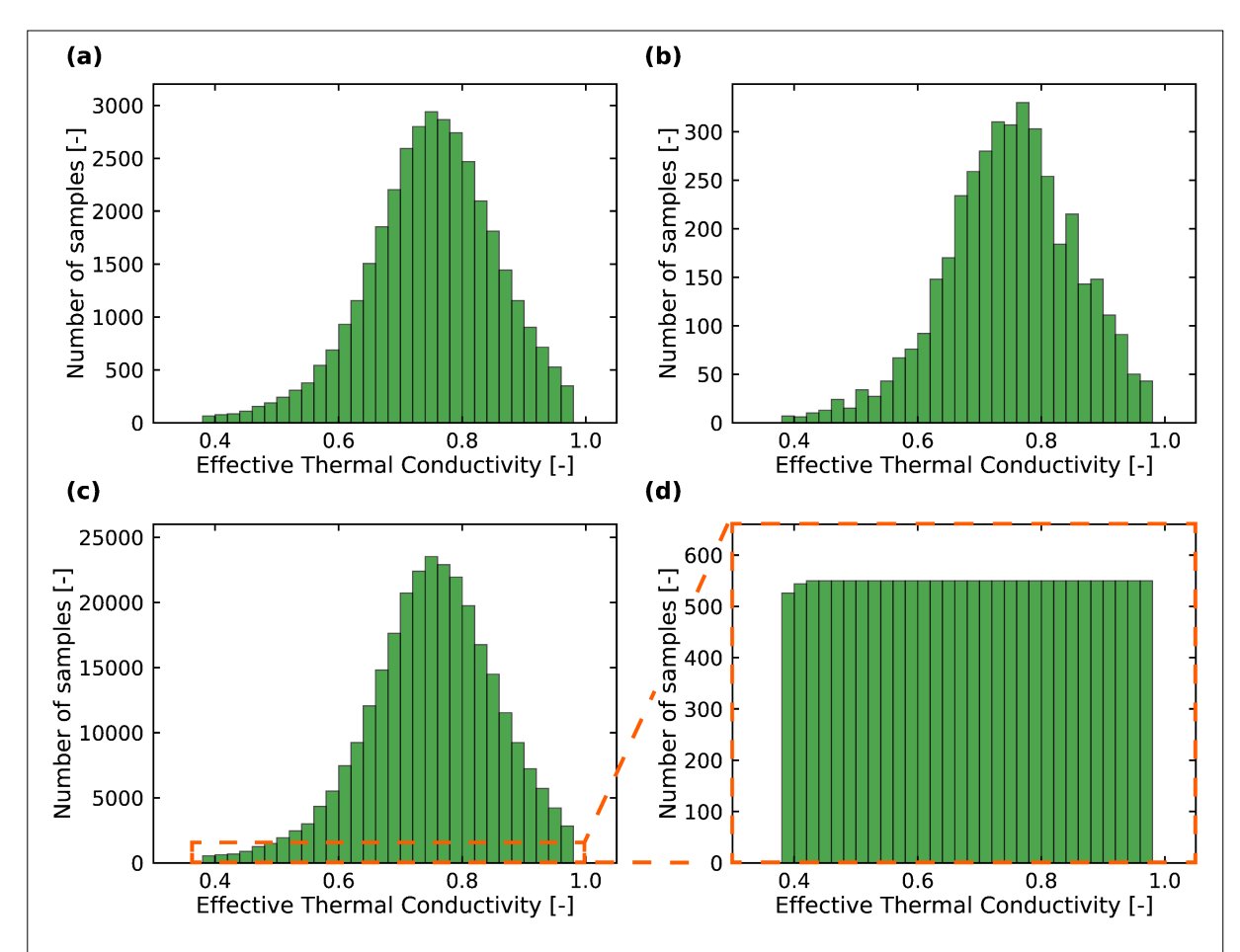


Figure 2: The distributions of effective thermal conductivity (ETC) for the (a) training and (b) testing datasets, each consisting of  $150 \times 150 \times 150$  cubic voxel volumes, are presented. c) The ETC distribution of the augmented training dataset exhibits skewness, with a tail extending into the lower ETC value region. d) To construct a balanced dataset, we randomly select 550 subvolumes from each 0.02 interval within the ETC range of  $\lambda_{\rm eff} \in [0.38, 0.98]$  from the augmented dataset.

the ability of machine learning models to learn effectively from imbalanced datasets (12). To mitigate this issue and construct a balanced dataset, we implemented an under-sampling strategy. Specifically, we divided the augmented dataset into bins corresponding to ETC intervals of 0.02 and randomly selected 550 subvolumes from each bin. This method yielded an evenly distributed dataset with ETC values from 0.38 to 0.98 (**Fig. 2d**), with the upper threshold indicating a lack of sufficient subvolumes beyond that point. The resulting balanced dataset, consisting of approximately 16,000 subvolumes, was then utilized for training the machine learning models and it was further split into training and validation subsets using the same 90-10 ratio applied during model training.

# 2.2. Transfer Learning and Pre-trained Models

Transfer learning is a machine learning technique that involves leveraging knowledge gained from a pretrained model on one task or domain to improve the performance of a model on a different but related task or domain. By reusing the weights of the pre-trained model, transfer learning accelerates the training process, enhances model performance, and reduces the need for large amounts of training data (71). This approach has been successfully applied across various fields, including computer vision (16, 28), natural language processing (4, 58), and speech recognition (43, 56).

There are two primary ways to apply transfer learning: fine-tuning and feature extraction. Fine-tuning involves using the weights of a pre-trained model as a starting point and re-training the model on a new dataset for a specific task, allowing the pre-trained weights to be adjusted or "fine-tuned" to perform well on the new task (27). In contrast, the feature extraction approach leverages the earlier layers (e.g., the initial convolutional layers) of the pre-trained model to extract relevant features from the new

Elmorsy et al. Page 8 of 19

dataset, while a newly added set of layers (e.g., the fully connected layers) is trained specifically for the target task using these extracted features. This method is particularly useful when the pre-trained model has already learned features that are applicable to the new task (71). In this study, we adopted the latter approach by employing four different pre-trained CNN models as feature extractors to develop new models for predicting the effective thermal conductivity (ETC) of 3D porous media. The pre-trained models were used strictly for feature extraction, not fine-tuning. Specifically, the feature extraction modules retained frozen weights throughout training, ensuring that the pre-trained layers acted solely as non-trainable feature extractors to identify relevant patterns in the input data. In contrast, the regression modules were composed of fully connected layers with randomly initialized weights, which were trained from scratch for the specific task of ETC prediction. This setup adheres to the standard definition of feature extraction, where pre-trained models provide stable, fixed features, and only the newly added layers are trained for the target application. We utilized the VGG16, ResNet50, and InceptionV3 models—2D CNN models pre-trained on the ImageNet dataset—along with a 3D CNN model pre-trained on a comprehensive digital rock dataset for permeability prediction (22). Below, we provide a more detailed description of the four pre-trained models.

The VGG16 model is a CNN trained on a collection of over 14 million images from the ImageNet dataset. Introduced by Simonyan and Zisserman (63), the VGG16 model achieved a top-5 accuracy of 91.1% in the 2014 ImageNet Large Scale Visual Recognition Challenge (ILSVRC) (59). To use the VGG16 model as a feature extractor for our dataset, we imported the model while excluding its classification module consisting of fully connected layers. We then fed the 3D images as a stack of 2D slices—where each slice represents an image channel—into the VGG16 feature extractor, which outputs a stack of extracted visual features. This three-dimensional feature stack was flattened and used as input for our newly developed regression module, which consists of two consecutive fully connected layers with 128 and 64 neurons, respectively. These layers are designed to uncover latent relationships from the extracted features. To prevent overfitting during the training process, we applied a dropout rate of 0.1 to the fully connected layers. We employed the rectified linear unit (ReLU) as the activation function for these layers, as it

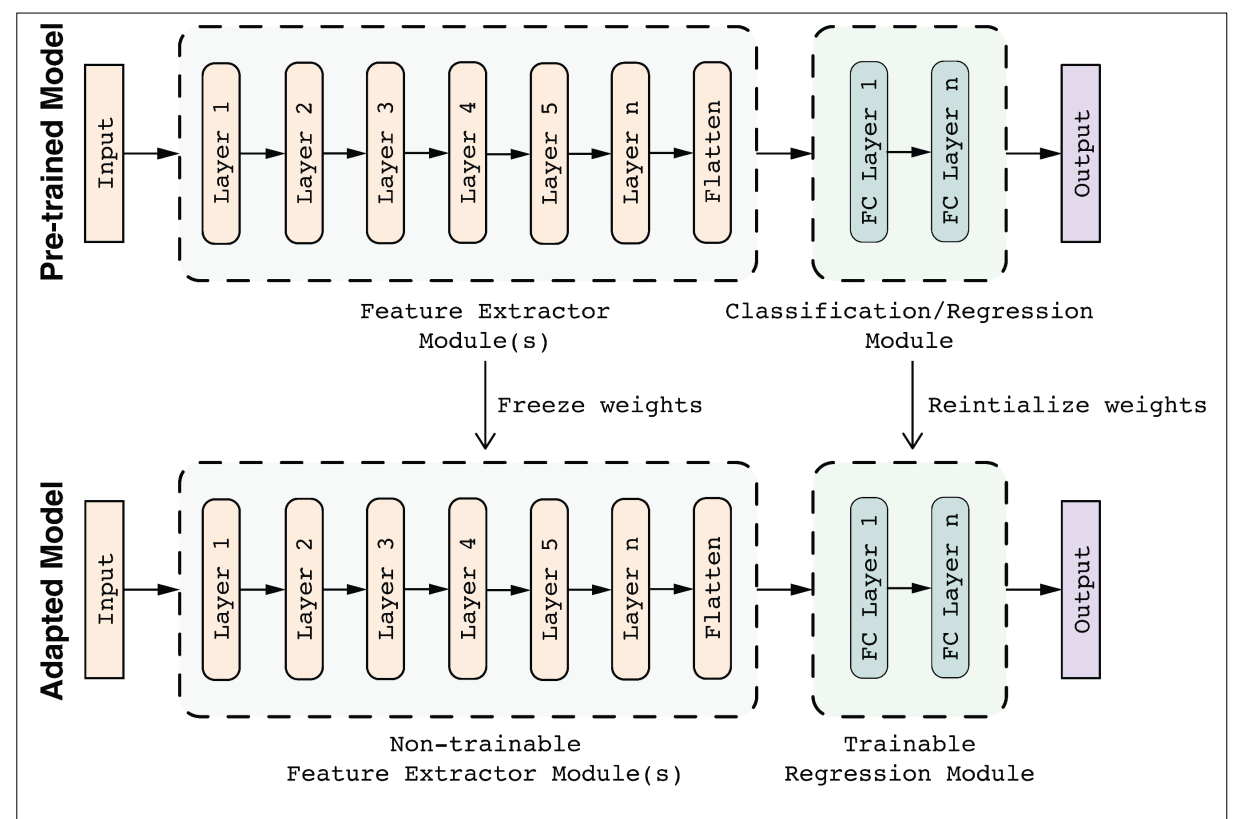


**Figure 3:** We apply transfer learning by using the earlier layers of pre-trained models as feature extractors, while training a new set of layers (i.e., the regression module) for our specific task of predicting effective thermal conductivity.

Elmorsy et al. Page 9 of 19

introduces non-linearity while minimizing computational cost (6). The final layer of the regression module is a single-neuron dense layer with a linear activation function that outputs the predicted ETC (**Fig. 3**).

The InceptionV3 model is the third generation of a deep CNN model that adopts an inception architecture. Introduced by researchers at Google, InceptionV3 has become a widely used image recognition model, demonstrating a top-5 accuracy of 93.9% on the ImageNet dataset (67). The model represents the integration of several advancements in deep learning architecture, as detailed by Szegedy et al. (67). The InceptionV3 architecture consists of several convolution layers, as well as layers for average pooling, max pooling, dropout, and a classification module that includes fully connected dense layers and a softmax activation function. For transfer learning, the final pooling layer, located just before the dense and softmax layers, is of particular interest. Thus, we imported the InceptionV3 model while excluding its classification module (i.e., top layers), allowing us to use it as a feature extractor. The extracted features were then fed into our newly developed regression module, which consists of two consecutive fully connected layers with 128 and 64 neurons, respectively, designed to uncover latent relationships within the features. The final layer of the regression module is a single-neuron dense layer with a linear activation function that outputs the predicted ETC (Fig. 3).

The ResNet50 model is a deep CNN and an expanded version of the ResNet model, a type of ANN that constructs networks by stacking residual modules—blocks of convolutional layers with shortcut connections. Developed by researchers at Microsoft, ResNet50 was trained on the ImageNet dataset and achieved a top-5 accuracy of 94.47% (32). ResNet50 is a 50-layer CNN comprising 48 convolutional layers, one max pooling layer, one average pooling layer, and a final fully connected dense layer with a SoftMax activation function. Similar to our approach with other models, we used the ResNet50 model as a feature extractor by importing the original model without its top layers. We then added our newly developed regression module, which consists of two consecutive fully connected layers with 128 and 64 neurons, respectively, designed to identify latent relationships within the extracted features. The final layer of the regression module is a single-neuron dense layer with a linear activation function that outputs the predicted ETC (Fig. 3).

Finally, we employed the multi-scale 3D CNN model introduced by Elmorsy et al. (22) for the prediction of digital rock permeability, referred to here as MS-PERM, in our transfer learning application. This model incorporates an inception module that consists of two parallel convolutional layer paths with varying kernel sizes, allowing for multi-scale feature aggregation. Following the inception module, a deep learning module further extracts deeper features, which are then passed to a final regression module capable of identifying latent relationships within the features and predicting permeability. The primary advantage of MS-PERM is that it was trained on one of the largest digital rock datasets available in the literature, comprising over 50,000 subvolumes of  $150 \times 150 \times 150$  voxels of digital porous media samples. Due to its novel architecture and the extensive dataset it was trained on, the model achieves excellent accuracy in predicting the permeability of various rock samples, with a mean absolute relative accuracy of 90.7%. In this study, we utilized MS-PERM as a feature extractor by importing the original model without its top layers. We then incorporated our newly developed regression module, consisting of two consecutive fully connected layers with 128 and 64 neurons, respectively, to uncover latent relationships from the extracted features. The regression module's final layer is a single-neuron dense layer with a linear activation function, which outputs the predicted ETC (Fig. 3).

We trained the four aforementioned models on a computing cluster equipped with four NVIDIA GeForce RTX 2080 Ti GPUs, using the open-source software interface Keras 2.4.0 and the machine learning library TensorFlow 2.3.1. The use of parallel computing enabled by GPUs significantly reduced training time and allowed the models to scale with additional resources (54). We use the mean squared error (MSE) as the loss function and train the model with the Adam optimizer, a computationally efficient variant of adaptive stochastic gradient descent (39).

We note that the regression models are designed to operate on a fixed input size (i.e.,  $150 \times 150 \times 150$  voxels). Given the memory-intensive nature of 3D CNNs, incorporating higher-resolution datasets would

Elmorsy et al. Page 10 of 19

introduce significant computational challenges. Downsampling the digital porous media samples may partially mitigate this issue; however, evaluating its effectiveness lies beyond the scope of the present study. Future work could explore the impact of downsampling on predictive accuracy by quantifying the trade-off between computational efficiency and the preservation of critical pore-scale features.

# 3. RESULTS AND DISCUSSION

We investigated the transfer learning methodology by training the four pre-trained models (i.e., VGG16, InceptionV3, ResNet50, MS-PERM) on the training dataset in two different scenarios: with and without pre-trained weights, each for 10 epochs. First, we trained the four models from scratch, starting with random initialization of all weights, including those in the feature extractor engine. In the second scenario, we trained the same models using frozen pre-trained weights for the feature extractor engine, while the weights of the regression module are trainable and initialized randomly in both cases. We assessed the performance of the trained models by evaluating prediction accuracy on the testing dataset and monitoring the training time. Prediction accuracy was measured by computing the absolute relative error (ARE) defined as  $ARE = |(\lambda_{eff}^{pred} - \lambda_{eff}^{true})/\lambda_{eff}^{true}|$ , where  $\lambda_{eff}^{pred}$  is the ETC predicted by the machine learning model,  $\lambda_{eff}^{true}$  is true ETC obtained from direct numerical simulation. To reduce the impact of outliers, we reported the model's accuracy solely for predictions with an ARE that falls within the 95<sup>th</sup> percentile.

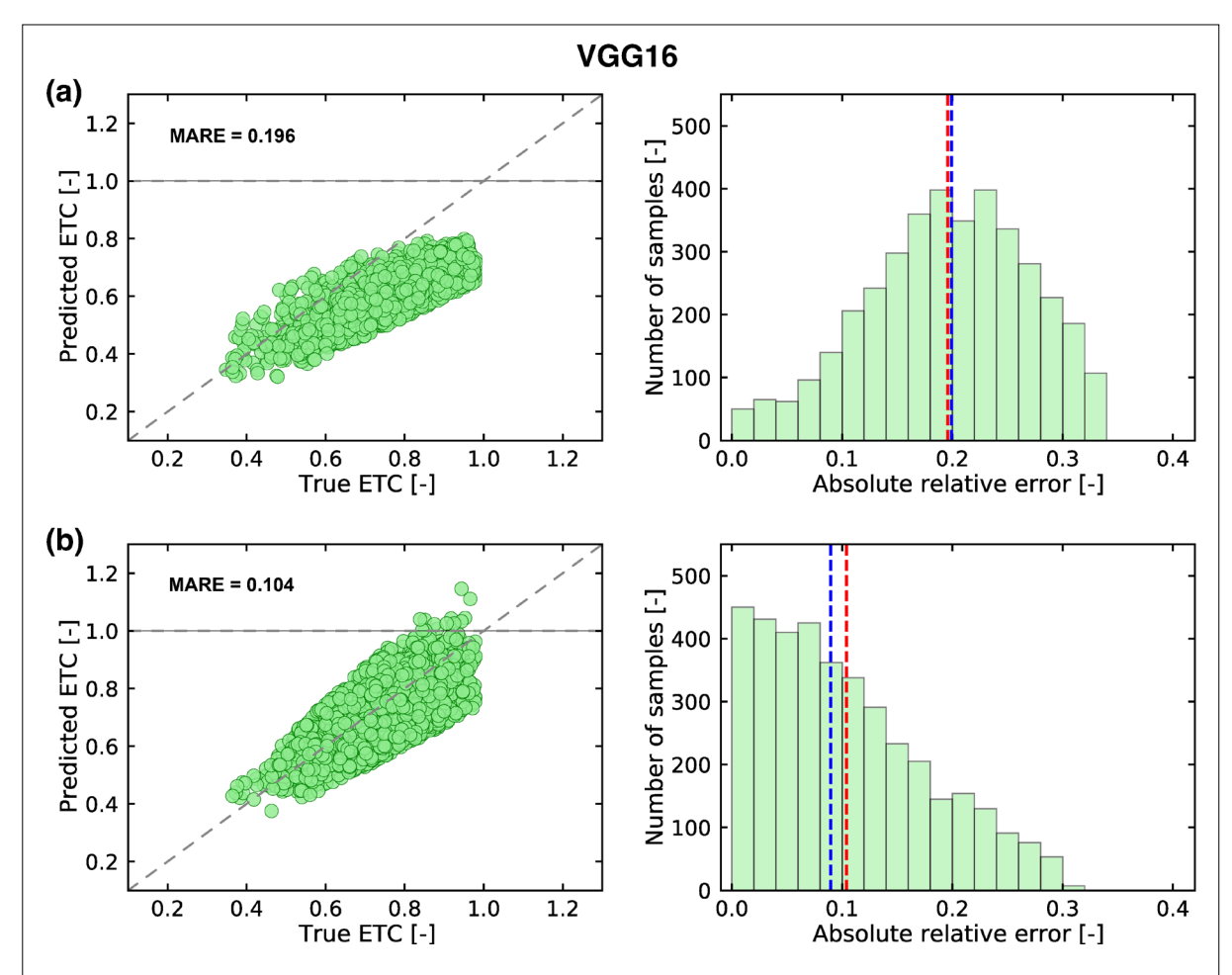


**Figure 4:** Effective thermal conductivity (ETC) prediction of the subvolumes from the testing dataset using **(a)** a VGG16 model trained from scratch and **(b)** a model trained with the pre-trained VGG16 feature extractor. The VGG16 model trained from scratch significantly underpredicts the true ETC, while the model trained with the pre-trained VGG16 feature extractor achieves excellent accuracy. The blue dashed vertical line represents the median ARE, while the red dashed line indicates the mean absolute relative error (MARE).

Elmorsy et al. Page 11 of 19

We began by assessing the predictive accuracy of the models based on VGG16. The VGG16 pre-trained model outperforms the VGG16 model trained from scratch, achieving a mean absolute relative error (MARE) of 0.104, which is significantly lower than the MARE of 0.196 achieved by the model trained from scratch (**Fig. 4**). We observed that the VGG16 model trained from scratch tends to underestimate the ETC values. Beyond accuracy enhancement, we found that the VGG16 pre-trained model is 2.4 times faster to train than the VGG16 model trained from scratch. This increased speed is primarily due to the reduced number of trainable parameters that need to be optimized and updated after each training epoch.

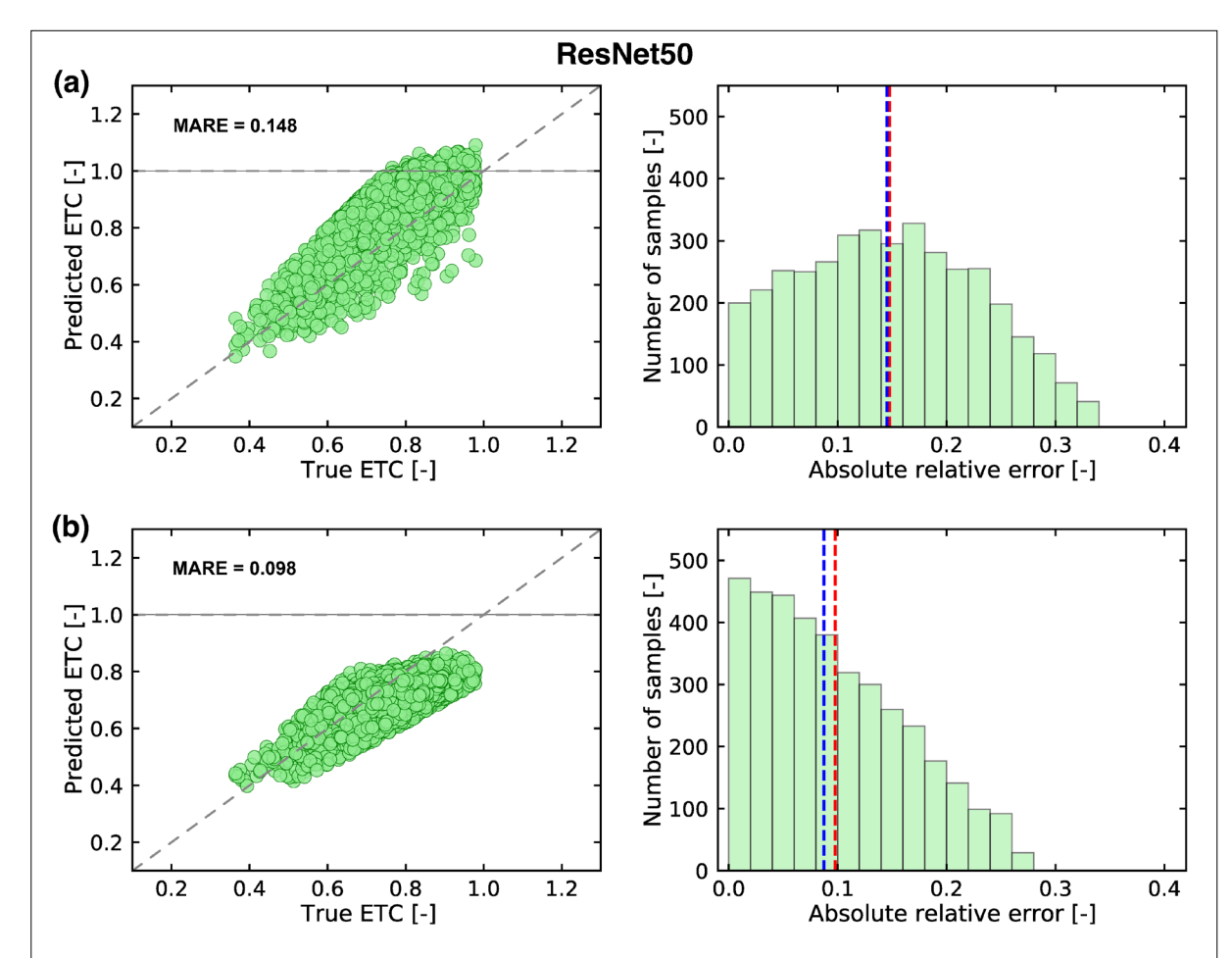


**Figure 5:** Effective thermal conductivity (ETC) prediction of the subvolumes from the testing dataset using **(a)** a ResNet50 model trained from scratch and **(b)** a model trained with the pre-trained ResNet50 feature extractor. The ResNet50 model trained from scratch overpredicts the true ETC, occasionally producing unphysical ETC values that are greater than one. The model trained with the pre-trained ResNet50 feature extractor achieves excellent accuracy. The blue dashed vertical line represents the median absolute relative error, while the red dashed line indicates the mean absolute relative error (MARE).

Next, we evaluated the models based on ResNet50. The evaluation revealed that the ResNet50 pre-trained model outperforms the ResNet50 model trained from scratch, with MARE values of 0.098 and 0.148, respectively (**Fig. 5**). We observed that the ResNet50 model trained from scratch tends to overestimate the ETC values, occasionally producing unphysical ETC values greater than one. In terms of training speed, we found that the ResNet50 pre-trained model was 3.3 times faster to train than the ResNet50 model trained from scratch, consistent with the trend observed with the VGG16 models.

Similarly, we evaluated the InceptionV3 models by quantifying their training and testing performance. We found that the InceptionV3 pre-trained model was significantly more accurate, achieving a MARE of 0.097 compared to 0.162 for the InceptionV3 model trained from scratch (**Fig. 6**). Additionally, the pre-trained model exhibited a reduced error distribution range (ARE  $\in$  [0,0.28]) compared to the broader

Elmorsy et al. Page 12 of 19

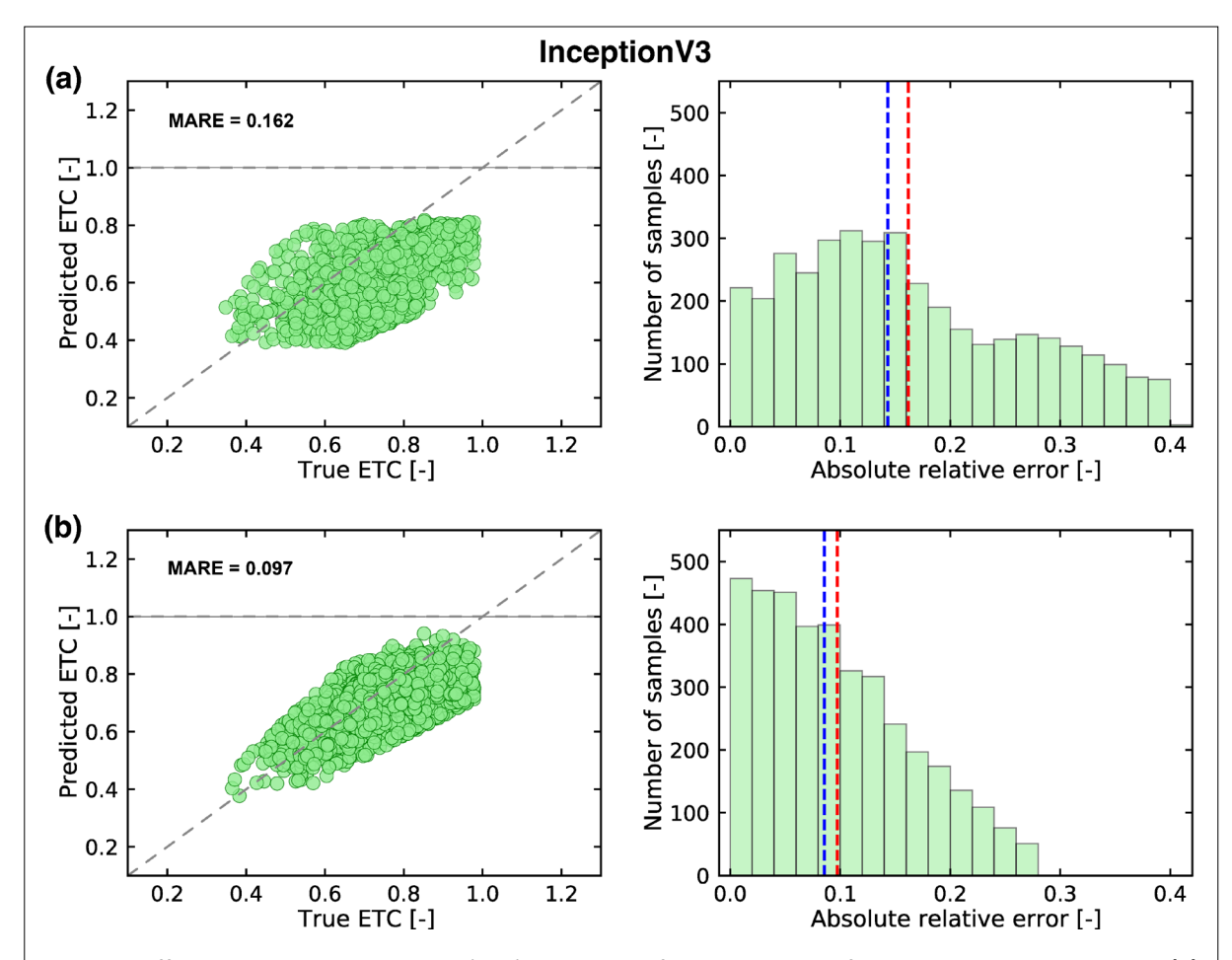


Figure 6: Effective thermal conductivity (ETC) prediction of the subvolumes from the testing dataset using (a) an InceptionV3 model trained from scratch and (b) a model trained with the pre-trained InceptionV3 feature extractor. The InceptionV3 model trained from scratch significantly underpredicts the true ETC, while the model trained with the pre-trained InceptionV3 feature extractor achieves excellent accuracy. The absolute relative error (ARE) of the InceptionV3 model trained from scratch has a wide distribution, whereas the ARE distribution for the model trained with the pre-trained InceptionV3 feature extractor is much narrower, with the majority of predictions concentrated in the low-error range. The blue dashed vertical line denotes the median ARE, while the red dashed line shows the mean absolute relative error (MARE).

range of ARE  $\in$  [0,0.4] observed for the model trained from scratch (**Fig. 6b**). The pre-trained model is also 3 times faster than the model trained from scratch for the same number of training epochs, highlighting the speed-up advantage of using pre-trained models.

Finally, we assessed the performance of the MS-PERM models. Our results indicate that the pre-trained MS-PERM model performed better, achieving a lower MARE of 0.090 compared to the MARE of 0.156 for the MS-PERM model trained from scratch (Fig. 7). The pre-trained MS-PERM model also outperformed all other models discussed earlier. This improvement is primarily attributed to the fact that the MS-PERM model was originally trained on a comprehensive 3D digital rock dataset, enabling its feature extractor to identify the most relevant features from the new dataset. Additionally, we found that the MS-PERM model trained from scratch tends to overestimate ETC values, occasionally producing unphysical ETC values greater than one. In contrast, the pre-trained MS-PERM model delivered balanced predictions across the entire ETC range (Fig. 7b). In fact, the pre-trained model exhibited the narrowest error distribution range among all models, with ARE values confined to [0, 0.26]. In terms of training speed, the pre-trained MS-PERM model was also 2.5 times faster than the MS-PERM model trained from scratch, reinforcing the advantage of using pre-trained models as feature extractors over training the entire model from scratch.

Elmorsy et al. Page 13 of 19

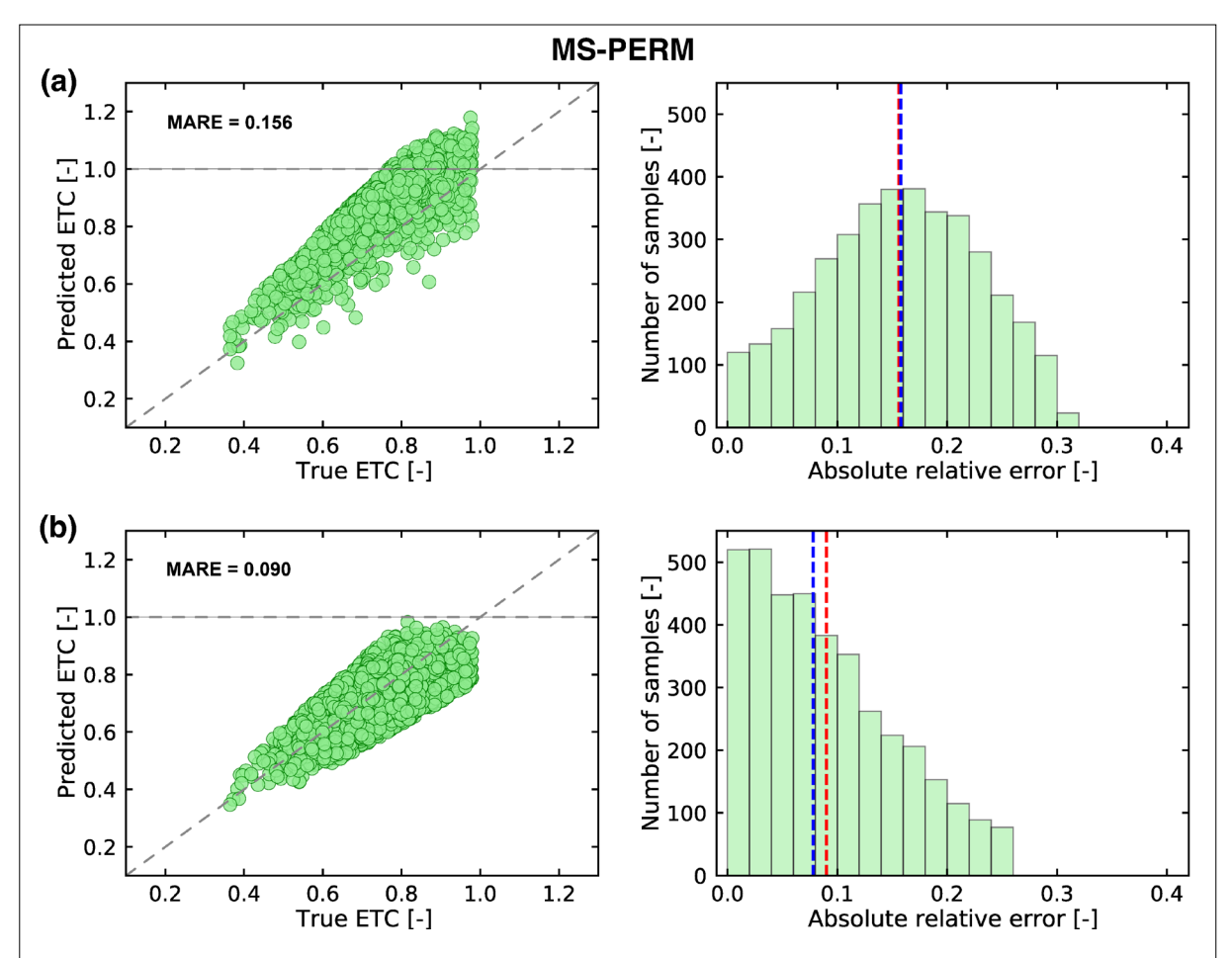


Figure 7: Effective thermal conductivity (ETC) prediction of the subvolumes from the testing dataset using (a) a MS-PERM model trained from scratch and (b) a model trained with the pre-trained MS-PERM model feature extractor. The MS-PERM model trained from scratch tends to overpredict the true ETC, occasionally producing unphysical ETC values greater than one, while the model leveraging the pre-trained MS-PERM feature extractor achieves excellent accuracy. Moreover, the model trained with the pre-trained MS-PERM feature extractor exhibits a narrower absolute relative error (ARE) range, with most predictions concentrated in the low-error range. The blue dashed vertical line represents the median ARE, while the red dashed line indicates the mean absolute relative error (MARE).

Our analysis clearly demonstrates the superior performance of pre-trained models employed as feature extractors compared to models trained from scratch, both in terms of prediction accuracy and training speed. Specifically, we show that using pre-trained models as feature extractors and training them on our target dataset results in predictions that are, on average, over 70% more accurate than those from models trained from scratch with random weight initialization. This technique proves highly advantageous in scenarios where large training datasets are unavailable, scarce, or time-consuming to compile. Similarly, in situations where large datasets are available but computational resources—such as memory or processing power—are limited, making it difficult to train models from scratch, pre-trained models offer a significant advantage. Furthermore, the pre-trained models are found to be, on average, 2.8 times faster to train than their counterparts trained from scratch. This speed advantage arises because pre-trained models, when used as feature extractors, require substantially fewer trainable parameters to be fine-tuned and optimized. This is especially beneficial when computational resources, like CPUs and GPUs, are constrained. These challenges—limited data availability, insufficient computational power, and time constraints—are common obstacles that many researchers face when training and fine-tuning machine learning models using traditional methods (82). By leveraging and expanding the application of transfer learning techniques in the domain of digital rock characterization, it will become increasingly Elmorsy et al. Page 14 of 19

feasible to predict, analyze, and understand various porous media properties (e.g., permeability, thermal conductivity, electrical resistivity, elastic modulus) with fewer resources and at higher speeds.

#### 4. CONCLUSION

In this study, we introduce a novel approach to digital porous media characterization by leveraging transfer learning. Our methodology effectively transfers prior knowledge from state-of-the-art machine learning models to significantly enhance both the speed and accuracy of new models tailored specifically for predicting the effective thermal conductivity (ETC) of digital porous media.

Our analysis focuses on the application of four pre-trained machine learning models—VGG16, ResNet50, InceptionV3, and MS-PERM—as feature extractors within machine learning models designed for end-to-end ETC predictions of  $150 \times 150 \times 150$  voxel subvolumes. The first three models, pre-trained on the ImageNet dataset, effectively extract generic image features, while the MS-PERM model, pre-trained on a comprehensive digital porous media dataset for permeability prediction, demonstrates superior ability in capturing specific features relevant to digital porous media. Despite utilizing a relatively modest training dataset of approximately 16,000 subvolumes, the models equipped with pre-trained feature extractors achieve remarkable accuracy on the testing dataset, with the MS-PERM model attaining the lowest mean absolute relative error (MARE) of 0.09. Our findings indicate that this enhanced accuracy is directly attributable to the adoption of transfer learning, which improves accuracy by over 70% compared to models trained from scratch. Additionally, the use of pre-trained models significantly increases computational efficiency, reducing training times by an average of 2.8 times.

Over the past decade, digital rock analysis has gained increasing significance in both academic research and industrial applications. Our work underscores the advantages of employing transfer learning techniques, particularly in scenarios where large training datasets are unavailable, scarce, or time-consuming to assemble, or where computational resources are limited. We anticipate that the continued application and expansion of transfer learning in porous media characterization will facilitate more effective, resource-efficient, and rapid predictions and analyses of key subsurface properties, including permeability, electrical resistivity, and elastic modulus, thereby expanding the applicability of digital rock physics in subsurface engineering.

# STATEMENTS AND DECLARATIONS

#### **Author Contributions**

M.E. and B.Z. designed research; M.E. performed research and analyzed data; W.E. and B.Z. acquired funding and supervised research; and M.E., W.E., and B.Z. wrote the paper.

#### **Conflicts of Interest**

The authors have no relevant financial or non-financial interests to disclose.

# Data, Code & Protocol Availability

The data used in this manuscript were obtained from the freely accessible Imperial College London online repository portal (14). Numerical simulations of the 3D porous media samples were performed using OpenFOAM, an open-source suite of solvers for CFD simulations (33). The machine learning model was trained using the open-source software Keras 2.4.0 and TensorFlow 2.3.1 on NVIDIA GeForce RTX 2080 Ti GPUs. All figures were created with Matplotlib 3.5.1, which is available under the Matplotlib license at <a href="https://matplotlib.org/">https://matplotlib.org/</a>. Part of the software (v.1.1) for data processing and the machine learning model associated with this manuscript is publicly available on GitHub at <a href="https://github.com/elmorsym1/Transfer-Learning-ETC-Predictions">https://github.com/elmorsym1/Transfer-Learning-ETC-Predictions</a>.

# **Funding Received**

This study was funded by the Natural Sciences and Engineering Research Council of Canada (NSERC) Discovery Grants (RGPIN-2019-07162) and the Canadian Nuclear Energy Infrastructure Resilience

Elmorsy et al. Page 15 of 19

under Systemic Risk (CaNRisk) - Collaborative Research and Training Experience (CREATE) program. Additional support from the INTERFACE Institute and the INViSionLab at McMaster University is greatly appreciated. The data will be made publicly accessible on the author's repository (https://github.com/elmorsym1).

# **ORCID IDs**

Mohamed Elmorsy Wael El-Dakhakhni Benzhong Zhao https://orcid.org/0000-0002-7983-6139
 https://orcid.org/0000-0001-8617-261X
 https://orcid.org/0000-0003-1136-9957

# **REFERENCES**

- Abdulagatova, Z., Abdulagatov, I. M., & Emirov, V. N. (2009). Effect of temperature and pressure on the thermal conductivity of sandstone. *International Journal of Rock Mechanics and Mining Sciences*, 46(6), 1055– 1071. https://doi.org/10.1016/j.ijrmms.2009.04.011
- 2. Albert, K., Franz, C., Koenigsdorff, R., & Zosseder, K. (2017). Inverse estimation of rock thermal conductivity based on numerical microscale modeling from sandstone thin sections. *Engineering Geology*, 231, 1–8. https://doi.org/10.1016/j.enggeo.2017.10.010
- 3. Ali, A. H., Mohanad G. Yaseen, Mohammad Aljanabi, & Saad Abbas Abed. (2023). Transfer learning: A new promising techniques. *Mesopotamian Journal of Big Data*, 2023, 29–30. https://doi.org/10.58496/MJBD/2023/004
- 4. Alyafeai, Z., AlShaibani, M. S., & Ahmad, I. (2020). *A survey on transfer learning in natural language processing* (No. arXiv:2007.04239). arXiv. https://doi.org/10.48550/arXiv.2007.04239
- Alzubaidi, L., Al-Amidie, M., Al-Asadi, A., Humaidi, A. J., Al-Shamma, O., et al. (2021). Novel transfer learning approach for medical imaging with limited labeled data. *Cancers*, 13(7), 1590. https://doi.org/10.3390/cancers13071590
- Alzubaidi, L., Zhang, J., Humaidi, A. J., Al-Dujaili, A., Duan, Y., et al. (2021). Review of deep learning: Concepts, CNN architectures, challenges, applications, future directions. *Journal of Big Data*, 8(1), 53. https://doi.org/10.1186/s40537-021-00444-8
- 7. Andrä, H., Combaret, N., Dvorkin, J., Glatt, E., Han, J., et al. (2013a). Digital rock physics benchmarks—Part I: Imaging and segmentation. *Computers & Geosciences*, 50, 25–32. https://doi.org/10.1016/j.cageo.2012.09.005
- 8. Andrä, H., Combaret, N., Dvorkin, J., Glatt, E., Han, J., et al. (2013b). Digital rock physics benchmarks—part II: Computing effective properties. *Computers & Geosciences*, *50*, 33–43. https://doi.org/10.1016/j.cageo.2012.09.008
- 9. Askari, R., Taheri, S., & Hejazi, S. H. (2015). Thermal conductivity of granular porous media: A pore scale modeling approach. *AIP Advances*, 5(9), 097106. https://doi.org/10.1063/1.4930258
- 10. Banerjee, P., & Kashyap, S. (2024). Unlocking transfer learning's potential in natural language processing: An extensive investigation and evaluation. *2024 International Conference on Advances in Computing Research on Science Engineering and Technology (ACROSET)*, 1–7. https://doi.org/10.1109/ACROSET62108.2024.10743260
- 11. Bauder, R. A., & Khoshgoftaar, T. M. (2018). The effects of varying class distribution on learner behavior for medicare fraud detection with imbalanced big data. *Health Information Science and Systems*, 6(1), 9. https://doi.org/10.1007/s13755-018-0051-3
- Bauder, R. A., Khoshgoftaar, T. M., & Hasanin, T. (2018). An empirical study on class rarity in big data. 2018 17th IEEE International Conference on Machine Learning and Applications (ICMLA), 785–790. https://doi.org/10.1109/ICMLA.2018.00125
- 13. Berg, C. F., Lopez, O., & Berland, H. (2017). Industrial applications of digital rock technology. *Journal of Petroleum Science and Engineering*, 157, 131–147. https://doi.org/10.1016/j.petrol.2017.06.074
- 14. Bijeljic, B., & Raeini, A. Q. (n.d.). *Micro-CT images and networks*. Imperial College London. Retrieved June 25, 2025, from https://www.imperial.ac.uk/engineering/departments/earth-science/research/research-groups/pore-scale-modelling/micro-ct-images-and-networks/
- 15. Blunt, M. J., Bijeljic, B., Dong, H., Gharbi, O., Iglauer, S., et al. (2013). Pore-scale imaging and modelling. *Advances in Water Resources*, 51, 197–216. https://doi.org/10.1016/j.advwatres.2012.03.003

Elmorsy et al. Page 16 of 19

16. Brodzicki, A., Piekarski, M., Kucharski, D., Jaworek-Korjakowska, J., & Gorgon, M. (2020). Transfer learning methods as a new approach in computer vision tasks with small datasets. *Foundations of Computing and Decision Sciences*, 45(3), 179–193. https://doi.org/10.2478/fcds-2020-0010

- 17. Byra, M. (2018). Discriminant analysis of neural style representations for breast lesion classification in ultrasound. *Biocybernetics and Biomedical Engineering*, 38(3), 684–690. https://doi.org/10.1016/j.bbe.2018.05.003
- 18. Byra, M., Styczynski, G., Szmigielski, C., Kalinowski, P., Michałowski, Ł., et al. (2018). Transfer learning with deep convolutional neural network for liver steatosis assessment in ultrasound images. *International Journal of Computer Assisted Radiology and Surgery*, 13(12), 1895–1903. https://doi.org/10.1007/s11548-018-1843-2
- 19. Demuth, C., Mendes, M. A. A., Ray, S., & Trimis, D. (2014). Performance of thermal lattice Boltzmann and finite volume methods for the solution of heat conduction equation in 2D and 3D composite media with inclined and curved interfaces. *International Journal of Heat and Mass Transfer*, 77, 979–994. https://doi.org/10.1016/j.ijheatmasstransfer.2014.05.051
- 20. Diersch, H.-J. G. (2014). Heat transport in porous media. In H.-J. G. Diersch, *FEFLOW* (pp. 673–709). Springer Berlin Heidelberg. https://doi.org/10.1007/978-3-642-38739-5\_13
- 21. Dongxing, D., Xu, Z., Chunhao, W., Jiaqi, L., Yinjie, S., & Yingge, L. (2021). Determination of the effective thermal conductivity of the porous media based on digital rock physics. *Geothermics*, 97, 102267. https://doi.org/10.1016/j.geothermics.2021.102267
- 22. Elmorsy, M., El-Dakhakhni, W., & Zhao, B. (2022). Generalizable permeability prediction of digital porous media via a novel multi-scale 3D convolutional neural network. *Water Resources Research*, 58(3), e2021WR031454. https://doi.org/10.1029/2021WR031454
- 23. Elmorsy, M., El-Dakhakhni, W., & Zhao, B. (2023). Rapid permeability upscaling of digital porous media via physics-informed neural networks. *Water Resources Research*, 59(12), e2023WR035064. https://doi.org/10.1029/2023WR035064
- 24. Farahani, A., Pourshojae, B., Rasheed, K., & Arabnia, H. R. (2020). A concise review of transfer learning. *2020 International Conference on Computational Science and Computational Intelligence (CSCI)*, 344–351. https://doi.org/10.1109/CSCI51800.2020.00065
- 25. Fei, W., Narsilio, G. A., & Disfani, M. M. (2021). Predicting effective thermal conductivity in sands using an artificial neural network with multiscale microstructural parameters. *International Journal of Heat and Mass Transfer*, 170, 120997. https://doi.org/10.1016/j.ijheatmasstransfer.2021.120997
- 26. Galvez, R. L., Bandala, A., Dadlos, E. P., & Vicerra, R. R. P. (n.d.). *Object detection using CNN | pdf | Artificial Neural Network | Computer Science*. Scribd. Retrieved June 25, 2025, from https://www.scribd.com/document/737186240/Object-Detection-Using-CNN
- 27. Goodfellow, I., Bengio, Y., & Courville, A. (n.d.). *Deep learning*. MIT Press. Retrieved June 25, 2025, from https://mitpress.mit.edu/9780262035613/deep-learning/
- 28. Gopalakrishnan, K., Khaitan, S. K., Choudhary, A., & Agrawal, A. (2017). Deep Convolutional Neural Networks with transfer learning for computer vision-based data-driven pavement distress detection. *Construction and Building Materials*, 157, 322–330. https://doi.org/10.1016/j.conbuildmat.2017.09.110
- 29. Greenberg, H. R., Blink, J. A., Sutton, M., Fratoini, M., & Ross, A. D. (2012, March 26). *Application of Analytical Heat Transfer Models of Multi-Layered Natural and Engineered Barriers in Potential High-Level Nuclear Waste Repositories*. WM2012 Conference, Phoenix, Arizona, USA. https://www.osti.gov/servlets/purl/1114696
- 30. Gupta, V., Choudhary, K., DeCost, B., Tavazza, F., Campbell, C., et al. (2024). Structure-aware graph neural network based deep transfer learning framework for enhanced predictive analytics on diverse materials datasets. *NPJ Computational Materials*, 10(1), 1. https://doi.org/10.1038/s41524-023-01185-3
- 31. Gupta, V., Choudhary, K., Tavazza, F., Campbell, C., Liao, W., et al. (2021). Cross-property deep transfer learning framework for enhanced predictive analytics on small materials data. *Nature Communications*, 12(1), 6595. https://doi.org/10.1038/s41467-021-26921-5
- 32. He, K., Zhang, X., Ren, S., & Sun, J. (2016). Deep residual learning for image recognition. *2016 IEEE Conference on Computer Vision and Pattern Recognition (CVPR)*, 770–778. https://doi.org/10.1109/CVPR.2016.90
- 33. Horgue, P., Soulaine, C., Franc, J., Guibert, R., & Debenest, G. (2015). An open-source toolbox for multiphase flow in porous media. *Computer Physics Communications*, 187, 217–226. https://doi.org/10.1016/j.cpc.2014.10.005

Elmorsy et al. Page 17 of 19

34. Huynh, B. Q., Li, H., & Giger, M. L. (2016). Digital mammographic tumor classification using transfer learning from deep convolutional neural networks. *Journal of Medical Imaging*, 3(3), 034501. https://doi.org/10.1117/1.JMI.3.3.034501

- 35. Jia, G. S., Tao, Z. Y., Meng, X. Z., Ma, C. F., Chai, J. C., & Jin, L. W. (2019). Review of effective thermal conductivity models of rock-soil for geothermal energy applications. *Geothermics*, 77, 1–11. https://doi.org/10.1016/j.geothermics.2018.08.001
- 36. Kamencay, P., Benco, M., Mizdos, T., & Radil, R. (2017). A new method for face recognition using convolutional neural network. *Advances in Electrical and Electronic Engineering*, 15(4), 663–672. https://doi.org/10.15598/aeee.v15i4.2389
- 37. Kamrava, S., Tahmasebi, P., & Sahimi, M. (2020). Linking morphology of porous media to their macroscopic permeability by deep learning. *Transport in Porous Media*, 131(2), 427–448. https://doi.org/10.1007/s11242-019-01352-5
- 38. Kasar, M. M., Bhattacharyya, D., & Kim, T. (2016). Face recognition using neural network: A review. *International Journal of Security and Its Applications*, 10(3), 81–100. https://doi.org/10.14257/ijsia.2016.10.3.08
- 39. Kingma, D. P., & Ba, J. (2014). *Adam: A method for stochastic optimization*. arXiv. https://doi.org/10.48550/ARXIV.1412.6980
- 40. Kiran, B. R., Sobh, I., Talpaert, V., Mannion, P., Sallab, A. A. A., et al. (2022). Deep reinforcement learning for autonomous driving: A survey. *IEEE Transactions on Intelligent Transportation Systems*, 23(6), 4909–4926. https://doi.org/10.1109/TITS.2021.3054625
- 41. Kora, P., Ooi, C. P., Faust, O., Raghavendra, U., Gudigar, A., et al. (2022). Transfer learning techniques for medical image analysis: A review. *Biocybernetics and Biomedical Engineering*, 42(1), 79–107. https://doi.org/10.1016/j.bbe.2021.11.004
- 42. Krizhevsky, A., Sutskever, I., & Hinton, G. E. (2017). ImageNet classification with deep convolutional neural networks. *Communications of the ACM*, 60(6), 84–90. https://doi.org/10.1145/3065386
- 43. Kunze, J., Kirsch, L., Kurenkov, I., Krug, A., Johannsmeier, J., & Stober, S. (2017). *Transfer learning for speech recognition on a budget*. arXiv. https://doi.org/10.48550/ARXIV.1706.00290
- 44. Labus, M., & Labus, K. (2018). Thermal conductivity and diffusivity of fine-grained sedimentary rocks. *Journal of Thermal Analysis and Calorimetry*, 132(3), 1669–1676. https://doi.org/10.1007/s10973-018-7090-5
- 45. Liang, X., Liu, Y., Chen, T., Liu, M., & Yang, Q. (2019). Federated transfer reinforcement learning for autonomous driving. arXiv. https://doi.org/10.48550/ARXIV.1910.06001
- 46. Liu, M., Ahmad, R., Cai, W., & Mukerji, T. (2023). Hierarchical homogenization with deep-learning-based surrogate model for rapid estimation of effective permeability from digital rocks. *Journal of Geophysical Research:* Solid Earth, 128(2), e2022JB025378. https://doi.org/10.1029/2022JB025378
- 47. Maes, J., & Menke, H. P. (2022). GeoChemFoam: Direct modelling of flow and heat transfer in micro-CT images of porous media. *Heat and Mass Transfer*, 58(11), 1937–1947. https://doi.org/10.1007/s00231-022-03221-2
- 48. Meshalkin, Y., Shakirov, A., Popov, E., Koroteev, D., & Gurbatova, I. (2020). Robust well-log based determination of rock thermal conductivity through machine learning. *Geophysical Journal International*, 222(2), 978–988. https://doi.org/10.1093/gji/ggaa209
- 49. Mostaghimi, P., Blunt, M. J., & Bijeljic, B. (2013). Computations of absolute permeability on micro-CT images. *Mathematical Geosciences*, 45(1), 103–125. https://doi.org/10.1007/s11004-012-9431-4
- 50. Muljadi, B. P., Blunt, M. J., Raeini, A. Q., & Bijeljic, B. (2016). The impact of porous media heterogeneity on non-Darcy flow behaviour from pore-scale simulation. *Advances in Water Resources*, 95, 329–340. https://doi.org/10.1016/j.advwatres.2015.05.019
- 51. Murison, J., Moosavi, R., Schulz, M., Schillinger, B., & Schröter, M. (2015). Neutron tomography as a tool to study immiscible fluids in porous media without chemical dopants. *Energy & Fuels*, 29(10), 6271–6276. https://doi.org/10.1021/acs.energyfuels.5b01403
- 52. Nabipour, I., Raoof, A., Cnudde, V., Aghaei, H., & Qajar, J. (2024). A computationally efficient modeling of flow in complex porous media by coupling multiscale digital rock physics and deep learning: Improving the tradeoff between resolution and field-of-view. *Advances in Water Resources*, 188, 104695. https://doi.org/10.1016/j.advwatres.2024.104695
- 53. Olson, D. L. (2004). Data set balancing. In Y. Shi, W. Xu, & Z. Chen (Eds.), *Data Mining and Knowledge Management* (Vol. 3327, pp. 71–80). Springer Berlin Heidelberg. https://doi.org/10.1007/978-3-540-30537-8\_8

Elmorsy et al. Page 18 of 19

54. Owens, J. D., Houston, M., Luebke, D., Green, S., Stone, J. E., & Phillips, J. C. (2008). GPU computing. *Proceedings of the IEEE*, 96(5), 879–899. https://doi.org/10.1109/JPROC.2008.917757

- 55. Popov, Y. A., Pribnow, D. F. C., Sass, J. H., Williams, C. F., & Burkhardt, H. (1999). Characterization of rock thermal conductivity by high-resolution optical scanning. *Geothermics*, 28(2), 253–276. https://doi.org/10.1016/S0375-6505(99)00007-3
- 56. Qin, C.-X., Qu, D., & Zhang, L.-H. (2018). Towards end-to-end speech recognition with transfer learning. *EURASIP Journal on Audio, Speech, and Music Processing*, 2018(1), 18. https://doi.org/10.1186/s13636-018-0141-9
- 57. Rong, Q., Wei, H., Huang, X., & Bao, H. (2019). Predicting the effective thermal conductivity of composites from cross sections images using deep learning methods. *Composites Science and Technology*, 184, 107861. https://doi.org/10.1016/j.compscitech.2019.107861
- 58. Ruder, S., Peters, M. E., Swayamdipta, S., & Wolf, T. (2019). Transfer learning in natural language processing. *Proceedings of the 2019 Conference of the North*, 15–18. https://doi.org/10.18653/v1/N19-5004
- 59. Russakovsky, O., Deng, J., Su, H., Krause, J., Satheesh, S., et al. (2015). ImageNet large scale visual recognition challenge. *International Journal of Computer Vision*, 115(3), 211–252. https://doi.org/10.1007/s11263-015-0816-y
- 60. Salehi, A. W., Khan, S., Gupta, G., Alabduallah, B. I., Almjally, A., et al. (2023). A study of CNN and transfer learning in medical imaging: Advantages, challenges, future scope. *Sustainability*, 15(7), 5930. https://doi.org/10.3390/su15075930
- 61. Sapińska-Śliwa, A., Sliwa, T., Twardowski, K., Szymski, K., Gonet, A., & żuk, P. (2020). Method of averaging the effective thermal conductivity based on thermal response tests of borehole heat exchangers. *Energies*, 13(14), 3737. https://doi.org/10.3390/en13143737
- 62. Shorten, C., & Khoshgoftaar, T. M. (2019). A survey on image data augmentation for deep learning. *Journal of Big Data*, 6(1), 60. https://doi.org/10.1186/s40537-019-0197-0
- 63. Simonyan, K., & Zisserman, A. (2014). *Very deep convolutional networks for large-scale image recognition.* arXiv. https://doi.org/10.48550/ARXIV.1409.1556
- 64. Singh, A., & Gosain, A. (2024). Catalyzing medical imaging: Exploring the potentials of deep transfer learning. *Journal of Information and Optimization Sciences*, 45(2), 439–448. https://doi.org/10.47974/JIOS-1561
- 65. Song, R., Liu, J., & Cui, M. (2017). A new method to reconstruct structured mesh model from micro-computed tomography images of porous media and its application. *International Journal of Heat and Mass Transfer*, 109, 705–715. https://doi.org/10.1016/j.ijheatmasstransfer.2017.02.053
- 66. Sreerama, J., & Sistla, S. M. K. (2023). Harnessing the power of transfer learning in deep learning models. *Journal of Knowledge Learning and Science Technology ISSN: 2959-6386 (Online)*, 1(1), 139–147. https://doi.org/10.60087/jklst.vol1.n1.p147
- 67. Szegedy, C., Vanhoucke, V., Ioffe, S., Shlens, J., & Wojna, Z. (2016). Rethinking the inception architecture for computer vision. *2016 IEEE Conference on Computer Vision and Pattern Recognition (CVPR)*, 2818–2826. https://doi.org/10.1109/CVPR.2016.308
- 68. Tajbakhsh, N., Shin, J. Y., Gurudu, S. R., Hurst, R. T., Kendall, C. B., et al. (2016). Convolutional neural networks for medical image analysis: Full training or fine tuning? *IEEE Transactions on Medical Imaging*, 35(5), 1299–1312. https://doi.org/10.1109/TMI.2016.2535302
- 69. Tong, F., Jing, L., & Zimmerman, R. W. (2009). An effective thermal conductivity model of geological porous media for coupled thermo-hydro-mechanical systems with multiphase flow. *International Journal of Rock Mechanics and Mining Sciences*, 46(8), 1358–1369. https://doi.org/10.1016/j.ijrmms.2009.04.010
- 70. Tong, Z., Liu, M., & Bao, H. (2016). A numerical investigation on the heat conduction in high filler loading particulate composites. *International Journal of Heat and Mass Transfer*, 100, 355–361. https://doi.org/10.1016/j.ijheatmasstransfer.2016.04.092
- Torrey, L. A., & Shavlik, J. W. (2009). Chapter 11: Transfer Learning. In Olivas, E. S., Guerrero, J. D. M., Sober, M. M., Benedito, J. R. M., & López, A. J. S (Eds.). *Handbook of Research on Machine Learning 36 Applications and Trends: Algorithms, Methods, and Techniques*. (pp. 242-264). Information Science Reference. https://doi.org/10.4018/978-1-60566-766-9.ch011 / https://doi.org/10.4018/978-1-60566-766-9
- Troch, A., Hoog, J. D., Vanneste, S., Balemans, D., Latré, S., & Hellinckx, P. (2022). Transfer learning in autonomous driving using real-world samples. In L. Barolli (Ed.), *Advances on P2P, Parallel, Grid, Cloud and Internet Computing* (Vol. 343, pp. 237–245). Springer International Publishing. https://doi.org/10.1007/978-3-030-89899-1\_24

Elmorsy et al. Page 19 of 19

73. Vaferi, B., Gitifar, V., Darvishi, P., & Mowla, D. (2014). Modeling and analysis of effective thermal conductivity of sandstone at high pressure and temperature using optimal artificial neural networks. *Journal of Petroleum Science and Engineering*, 119, 69–78. https://doi.org/10.1016/j.petrol.2014.04.013

- 74. Von Herzen, R., & Maxwell, A. E. (1959). The measurement of thermal conductivity of deep-sea sediments by a needle-probe method. *Journal of Geophysical Research*, 64(10), 1557–1563. https://doi.org/10.1029/JZ064i010p01557
- 75. Wei, H., Bao, H., & Ruan, X. (2020). Machine learning prediction of thermal transport in porous media with physics-based descriptors. *International Journal of Heat and Mass Transfer*, 160, 120176. https://doi.org/10.1016/j.ijheatmasstransfer.2020.120176
- 76. Wei, H., Zhao, S., Rong, Q., & Bao, H. (2018). Predicting the effective thermal conductivities of composite materials and porous media by machine learning methods. *International Journal of Heat and Mass Transfer*, 127, 908–916. https://doi.org/10.1016/j.ijheatmasstransfer.2018.08.082
- 77. Weiss, K., Khoshgoftaar, T. M., & Wang, D. (2016). A survey of transfer learning. *Journal of Big Data*, 3(1), 9. https://doi.org/10.1186/s40537-016-0043-6
- 78. Wu, H., Fang, W.-Z., Kang, Q., Tao, W.-Q., & Qiao, R. (2019). Predicting effective diffusivity of porous media from images by deep learning. *Scientific Reports*, 9(1), 20387. https://doi.org/10.1038/s41598-019-56309-x
- 79. Yang, H., Zhang, L., Liu, R., Wen, X., Yang, Y., et al. (2019). Thermal conduction simulation based on reconstructed digital rocks with respect to fractures. *Energies*, 12(14), 2768. https://doi.org/10.3390/en12142768
- 80. Zahasky, C., & Benson, S. M. (2018). Micro-positron emission tomography for measuring sub-core scale single and multiphase transport parameters in porous media. *Advances in Water Resources*, 115, 1–16. https://doi.org/10.1016/j.advwatres.2018.03.002
- 81. Zeng, Y., Ji, B., Zhang, Y., Feng, J., Luo, J., & Wang, M. (2022). A fractal model for effective thermal conductivity in complex geothermal media. *Frontiers in Earth Science*, 10, 786290. https://doi.org/10.3389/feart.2022.786290
- 82. Zhang, J., Ma, G., Yang, Z., Mei, J., Zhang, D., et al. (2024). Knowledge extraction via machine learning guides a topology-based permeability prediction model. *Water Resources Research*, 60(7), e2024WR037124. https://doi.org/10.1029/2024WR037124
- 83. Zhang, Y., Hao, S., Yu, Z., Fang, J., Zhang, J., & Yu, X. (2018). Comparison of test methods for shallow layered rock thermal conductivity between in situ distributed thermal response tests and laboratory test based on drilling in northeast China. *Energy and Buildings*, 173, 634–648. https://doi.org/10.1016/j.enbuild.2018.06.009
- 84. Zhiqiang, W., & Jun, L. (2017). A review of object detection based on convolutional neural network. *2017 36th Chinese Control Conference (CCC)*, 11104–11109. https://doi.org/10.23919/ChiCC.2017.8029130